Available online at www.sciencedirect.com
SCIENCE DIRECT
Catalysis Today 107–108 (2005) 323–329
CATALYSIS TODAY
www.elsevier.com/locate/cattod

Cr, Mo and W used as VPO promoters in the partial oxidation of *n*-butane to maleic anhydride

Beatriz T. Pierini, Eduardo A. Lombardo *

Instituto de Investigaciones en Catálisis y Petroquímica, INCAPE (FIQ, UNL-CONICET), Santiago del Estero 2829, 3000 Santa Fe. República, Argentina

Available online 18 August 2005

Abstract

The present work addresses the issue of the promoter effect produced by group VIB elements added to the basic VPO formulation using different methods and loads in order to obtain information linking the catalytic behavior of the solids with their physicochemical properties. The unpromoted VPO precursor ($VOHPO_4{\cdot}1/2H_2O$) was prepared from V_2O_5 reduced with an alcoholic mixture and 100% H_3PO_4. Cr, Mo or W were either impregnated on the VPO precursor or co-precipitated during the precursor synthesis. The precursors containing varying loads of the promoter were activated following a standard procedure in the same flow micro-reactor where the catalytic performance was evaluated. The precursors and the catalysts were characterized by X-ray diffraction (XRD) and laser Raman spectroscopy (LRS). Acetonitrile was used as a probe molecule to test the strength of the Lewis acid sites monitored by FTIR. The amount of chemisorbed acetonitrile was measured in a standard high vacuum system. The addition of the promoters invariably increased the catalytic activity but in every case there was an optimum load to achieve the best selectivity. The origin of this maximum could be ascribed to the right balance between the presence of very strong Lewis acid sites and the development of V^{5+} isolated sites in the matrix of the vanadyl pyrophosphate, by far the major crystalline phase present in the catalyst. The three group VIB promoters affect the balance between acid and redox properties but increase the overall activity in all cases.

Keywords: VPO; Promoters; Partial oxidation; Maleic anhydride; Cr; Mo; W

1. Introduction

The mixed phosphorus and vanadium oxide known as VPO is the only system capable of oxidizing *n*-butane to maleic anhydride with good selectivity. Promoters are added to industrial formulations to improve both catalytic properties and mechanical resistance. A long list of elements has been tested but the exact role of each element is mostly unknown and controversial.

Different authors have stressed a variety of aspects concerning the role of promoters such as the mode of addition [1], the load [2], the promoter electronegativity [3], the generation of defects [4], the redox character [5] and acidity [6,7]. Other authors have speculated on the formation of a solid solution, based on the fact that molybdenum phosphate ($MoOPO_4$) and $VOPO_4$ are iso-structural phases and, consequently, it is possible that during the stabilization period a small amount of a solid solution of Mo and V mixed phase could have been formed [8]. More recent studies have used Mo in combination with other dopants (Zn, Zr) added by impregnation. Besides, in order to increase the surface area the precursors were ball milled [9].

Note that commercial catalysts always have P/V ratios slightly higher than one. Another alternative would be that the added metal forms some amorphous phase with excess phosphorus decreasing the loss of this element by sublimation, which requires its permanent replenishment in industrial practice [8]. Mc Cormick et al. [10] have proposed that a possible role of the promoter would be to accelerate the rate of V^{5+} phase formation to yield the neighboring V^{5+}/V^{4+} couples required in the Mars and van

* Corresponding author. Tel.: +54 342 4536861; fax: +54 342 4536861.
E-mail address: nfisico@fiqus.unl.edu.ar (E.A. Lombardo).

0920-5861/$ – see front matter © 2005 Elsevier B.V. All rights reserved.
doi:10.1016/j.cattod.2005.07.084

Krevelen [11] type of mechanism proposed for several steps of the overall reaction.

From a mechanistic viewpoint, it is well known that the hydrogen abstraction is the rate-determining step both in an olefinic and in an alcoxide mechanism [12–14]. A suitable candidate to favor the hydride abstraction is a strong Lewis site. According to Centi et al. [12], this site could be a $V^{4+\delta+}$ site stemming from defects in the structure of the vanadyl pyrophosphate [2 0 0] plane or, as suggested by Volta and co-workers, it could be a V^{5+} center either dispersed in the same phase or from a $VOPO_4$ phase [4,13,14].

The present work addresses the promoter effect produced by chromium, molybdenum and tungsten which have been added using different methods and loads in order to obtain information linking catalytic behavior of the solids with their physicochemical properties. These elements were selected because, similarly to V, they have a ''d'' character, various oxidation states under reaction conditions, their oxides are acidic and they could possibly form intercalation or substitution compounds with vanadium. Moreover, these elements are used in the oxidehydrogenation of short-chain paraffins where their main role is to accelerate the rate-determining step of C–H bond breaking [15,16].

2. Experimental

2.1. Precursor synthesis

The precursor was obtained by reduction of 5 g of V_2O_5 with 30 ml of isobutyl alcohol and 20 ml of benzyl alcohol under reflux for 3 h. Orthophosphoric acid 100% was then added in the amount needed to obtain a P/V ratio of 1.3 and the solution refluxed for another 2 h. After completion of the reaction, the solid phase was recovered by filtration and dried in an oven at 150 °C overnight. The solid obtained was the VPO catalyst precursor (with no promoter added). Two types of promoted catalysts were prepared: (i) impregnated and (ii) co-precipitated. In order to prepare the impregnated formulations, the necessary amount of isobutyl alcohol solution of the corresponding salt was incorporated to the VPO precursor by incipient wetness technique. In the case of co-precipitated solids, the salt containing the promoter was also dissolved in isobutyl alcohol and added to the system in the phosphatation step together with the phosphoric acid.

A VPO(a) base was prepared to impregnate Mo with 1.0, 3.0 and 5.0% and a second VPO(b) base was also prepared for the impregnation of Cr and W, yielding catalysts impregnated with 0.5, 1.0 and 1.5% Cr and with 1.7, 3.5 and 10.5% W. The co-precipitated catalysts had 1.0 and 5.0% Mo; 1.0, 1.5 and 3.0% Cr and 2.5, 5.0 and 10.5% W. The nomenclature used is M/%/x, to indicate promoter name/metal% by weight/x: preparation method, where i: impregnation and c: co-precipitation. The promoter concentrations were calculated through a mass balance made taking into account the amount of reactants used in the preparation. This is justified by the fact that the promoter salts accurately weighted are fully incorporated in the precursor with no residues left out.

2.2. Catalyst activation and testing

A fixed-bed reactor containing 1.0 g of precursor with particle size in the range of 177–250 microns was used to activate the solids and perform the catalytic tests. *n*-Butane and maleic anhydride were analyzed using an on-line gas chromatograph equipped with an FID detector and an AT-1200 column. The precursor was activated as follows: while flowing the reactant mixture (1.5% *n*-C_4H_{10} in air) at GHSV = 900 h^{-1}, the solid was heated at 3 °C min^{-1}, up to 280 °C, kept at this temperature for 3 h and heated again to the temperature needed to achieve 80% conversion (∼380 °C). The system was kept under reaction conditions until no variation in both conversion and selectivity occurred (usually 48 h). At this point, the catalyst reached the steady state to measure its catalytic performance by varying temperature and space velocity as needed.

2.3. Precursor and catalyst characterization

2.3.1. Surface area

It was measured by N_2 adsorption (BET method) using a Quantachrome Nova 1000 sorptometer.

2.3.2. X-ray diffraction (XRD)

The measurements were made with a Shimadzu XD-D1 X-ray diffractometer, using nickel-filtered Cu Kα radiation with a scanning rate of 1° min^{-1}.

2.3.3. Laser Raman spectroscopy (LRS)

The Raman spectra were recorded with a Jasco laser Raman spectrometer model TRS-600-SZ-P, equipped with a charge coupled device (CCD) with the detector cooled to about 153 K using liquid N_2. The excitation source was the 514.5 nm line of a spectra 9000 photometrics Ar ion laser. The laser power was set at 40 mW. The powdered solid was pressed as a thin wafer about 1 mm thick, and all the spectra were recorded with the samples under ambient conditions.

2.3.4. Fourier transform infrared spectroscopy

The IR spectra were obtained using a Shimadzu FT-IR 8101M spectrometer with a spectral resolution of 4 cm^{-1}.

2.3.5. Acetonitrile adsorption

The samples for the adsorption experiments were prepared by compressing the used catalysts at 4 tonnes cm^{-2} 2 in order to obtain self-supporting wafers. They were mounted on a transportable infrared cell with CaF_2 windows and external oven. The pretreatment was performed in a high vacuum system. The sample was first outgassed at 450 °C for 12 h in a dynamic vacuum of 1.0×10^{-5} Torr. After cooling to room temperature, a spectrum of the catalyst

wafer was taken. This spectrum is very important, because it was later going to be subtracted from the subsequent spectra. Then, acetonitrile (30 Torr) was adsorbed on the solid and the spectrum was taken.

No bands were observed in the 1600 cm^{-1} region; therefore, no water was introduced during acetonitrile adsorption. Spectra were also recorded after adsorption at 30 °C and after evacuation of the cell for 10 min at 30, 80 and 150 °C, respectively.

2.3.6. Chemisorption of acetonitrile

One hundred milligrams of catalyst were charged in the reactor and then the sample was out-gassed at 450 °C overnight. Following calibration of the dead volumes by He, the amount of chemisorbed acetonitrile was measured in a standard high vacuum system.

3. Results and discussion

3.1. Structure of precursors and catalysts

The diffractograms of all the precursors (not shown) indicate that the only crystalline phase is the hemihydrated vanadyl hydrogen phosphate, $VOHPO_4 \cdot 1/2H_2O$. The surface area of the unpromoted VPO and those containing either Cr or Mo were ca. 12 $m^2\ g^{-1}$. Those containing W had a surface area between 2 and 7.5 $m^2\ g^{-1}$. In all the catalysts with a BET area between 13 and 56 $m^2\ g^{-1}$ the predominant and sometimes excluding phase was vanadyl pyrophosphate, $(VO)_2P_2O_7$. Fig. 1 shows the diffractograms of the best performing formulations and only one of the VPO bases since both have the same patterns. Note that all but the Cr1.0i catalyst only show the fingerprints of vanadyl pyrophosphate. The Cr-containing solid also shows the presence of two V^{5+} phases: γ-$VOPO_4$ and $VOPO_4 \cdot 2H_2O$. We have also

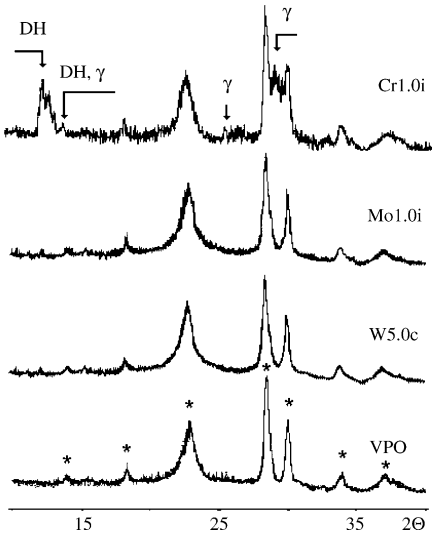

Fig. 1. XRD patterns of the best promoted catalysts and the unpromoted formulations. (*) Vanadyl pyrophosphate reflections.

carefully searched the diffractograms of the 17 promoted catalysts under study trying to discover the presence of segregate phases which could contain the promoter without success. The main phases searched for were the corresponding promoter oxides and phosphates. This of course does not discard the formation of either amorphous or surface compounds. Gai and Kourtakis [17] found that the incorporation of additives to $(VO)_2P_2O_7$ produces glide shear defects associated with anionic vacancies which do not modify the VPO bulk structure and which are undetectable by XRD. For this reason, Raman spectroscopy, more sensitive to the presence of phases and/or V^{5+} dispersed species, is used in their studies [18].

The most relevant structural features of the precursors and catalysts of the best performing formulations are reported in Table 1. Several authors [12,17,19,20] have suggested that the structural features of the promoters (e.g. the presence of defects) directly influence those of the catalysts. Since defects are connected with the generation of very strong Lewis acid sites, the catalytic behavior of the solids should also be connected with the extent of structural disorder of the precursor [17]. The fifth and sixth columns of Table 1 show no correlation between the corresponding planes in the precursor and the catalyst. Furthermore, no correlation was either found in the 18 precursor–catalyst couples studied here (data not shown). This finding is not surprising because during the phase transformation, the solid becomes amorphous and the new crystalline pyrophosphate phase develops with time on stream [21].

The addition of these promoters did not significantly modify the vanadyl pyrophosphate structure since: (i) the FWHM of the [2 0 0] plane was not systematically affected by promoter addition (Table 1) and (ii) the unit cell volume was in the 18 cases ∼1230 $Å^3$. It is clear, however, that defects located at the surface could not be detected through XRD.

Two distinctive effects of Cr and Mo are depicted in Table 1: (i) the former element increases the surface area of the catalyst (Table 1) and (ii) Mo1.0i is the only one to show a preferential exposure of the [2 0 0] plane which is unanimously accepted [12,20,22] as the loci of active sites for the oxidation of *n*-C_4H_{10} to maleic anhydride. All the Cr-containing catalysts have surface areas between 35 and 48 $m^2\ g^{-1}$ while all the others only have 13–22 $m^2\ g^{-1}$. Note, however, that the surface area of the Cr catalysts is affected by neither the load nor the method of preparation. Concerning the [2 0 0] plane exposure, all the Mo-containing catalysts show I[2 0 0]/I[0 4 2] ratios between 0.63 and 0.95 with no correlation with either load or method of preparation.

3.2. Catalytic behavior

Table 2 shows a summary of the catalytic performance of the 18 formulations synthesized and assayed. The T_{80} column indicates the temperature needed to reach 80%

Table 1
Structural and textural properties of the best precursors and catalysts

Solid	M/V[a] × 10^2	BET area (m^2/g)		Precursor FWHM [0 0 1]	Catalyst FWHM [2 0 0]	Intensity ratio (DRX)	
		Precursor	Catalyst			Precursor I[0 0 1]/I[2 2 0]	Catalyst I[2 0 0]/I[0 4 2]
VPO(a)	–	11.1	21.8	1.063	1.236	0.25	0.53
Mo1.0i	1.8	11.0	22.0	0.933	1.146	0.25	0.69
VPO(b)	–	11.0	28.2	0.994	1.339	0.25	0.53
Cr1.0i	3.6	13.0	46.2	0.277	1.211	0.41	0.52
W5.0c	5.4	2.8	26.2	1.326	1.193	0.25	0.52

[a] Promoter (M)/vanadium (V) atomic ratio.

conversion, while the S_{80} shows the selectivity at this conversion level. The 80% conversion mark was not surpassed during the tests to protect the catalysts from a highly oxidizing atmosphere which could cause its over-oxidation and consequent deterioration.

The first observation from Table 2 is that all the promoted formulations are more active than the unpromoted VPO, i.e. T_{80} is always lower than 445 °C. On the other hand, the promoted catalysts can be more or less selective than VPO depending on the nature of the promoter, its load and the method of preparation. Note that the impregnated catalysts containing Cr and Mo are in general more selective than the co-precipitated ones. The reverse is true for W.

Fig. 2 shows the catalytic behavior of the three best promoted catalysts and the two bases employed to prepare the impregnated formulations. Mo was the element which produced the most active and selective catalyst. Its high activity at low temperatures should be remarked since it allows operation at lower temperatures. The fact that Cr is also a good promoter at the 1% level is not in agreement with what Harrouch Batis et al. [1] reported for VPO catalysts doped with Cr (in loads similar to ours). These authors found that the promoting effect did not occur and that, on the contrary, the selectivity to maleic anhydride deteriorated, furane proportions increased at low conversion and CO proportions increased at high conversions. However, it should be noted that our preparation is organic and the addition is performed by impregnation of $Cr(NO_3)_2{\cdot}9H_2O$ dissolved in isobutyl alcohol, whereas they used a simultaneous addition of $CrCl_3$ to an aqueous solution of $VCl_3 + V_2O_5$ to which they later added phosphoric acid. This proves that both the preparation method and the way the promoter is added strongly affect the final result.

The W5.0c was in between Mo1.0i and Cr1.0i both in activity and selectivity. The W used as promoter of the VPO system is mentioned in numerous patents but its catalytic behavior is unknown in the open literature. Note that VPO(a) and VPO(b) differ in activity but not in selectivity.

3.3. LRS data

This technique is more sensitive than XRD to detect the presence of minority phases in the VPO system. It confirmed that the vanadyl pyrophosphate was the majority phase in all catalysts and the exclusive one in several of them. In Fig. 3, it is seen that W5.0c and VPO(a) only exhibit the fingerprints of the pyrophosphate at 1178, 1134, 1125 and 923 cm^{-1} [23,24]. The same is true for VPO(b) (not shown). In the case of Mo1.0i, this technique detected the presence of α_I-$VOPO_4$ not seen in the XRD profile (Fig. 1). In the case of Cr1.0i, it also confirmed the presence of γ-$VOPO_4$ detected through XRD.

The main Raman band at 923 cm^{-1} has a FWHM of 21–22 cm^{-1} in the unpromoted VPO. We synthesized a stoichiometric well-crystallized $(VO)_2P_2O_7$ and measured

Table 2
Summary of catalytic behavior of all the formulations[a]

Catalysts	M/V × 10^2	T_{80}[b] (°C)	S_{80}[b] (%)	Catalysts	M/V × 10^2	T_{80}[b] (°C)	S_{80}[b] (%)
VPO	–	445	50				
Impregnated				Co-precipitated			
Cr0.5i	1.8	440	50	Cr1.0c	3.6	430	23
Cr1.0i	3.6	427	70	Cr1.5c	5.4	435	53
Cr1.5i	5.4	405	43	Cr3.0c	10.7	440	25
Mo1.0i	1.8	358	84	Mo1.0i[c]	1.8	375	0
Mo3.0i	5.9	370	50				
Mo5.0i[c]	9.9	382	22	Mo5.0c[c]	9.9	425	9
W1.7i	1.8	370	22	W2.5c	2.6	440	75
W3.5i	3.6	387	39	W5.0c	5.2	410	80
W10.5i	10.7	402	40	W10.5c	10.7	385	58

[a] The activation procedure and the catalytic test were carried out using 1.5% n-butane in air and GHSV: 900 h^{-1}.
[b] T_{80}, temperature to achieve 80% conversion; S_{80}: selectivity at 80% conversion.
[c] Tested with 0.8% n-butane in air and GHSV: 900 h^{-1}.

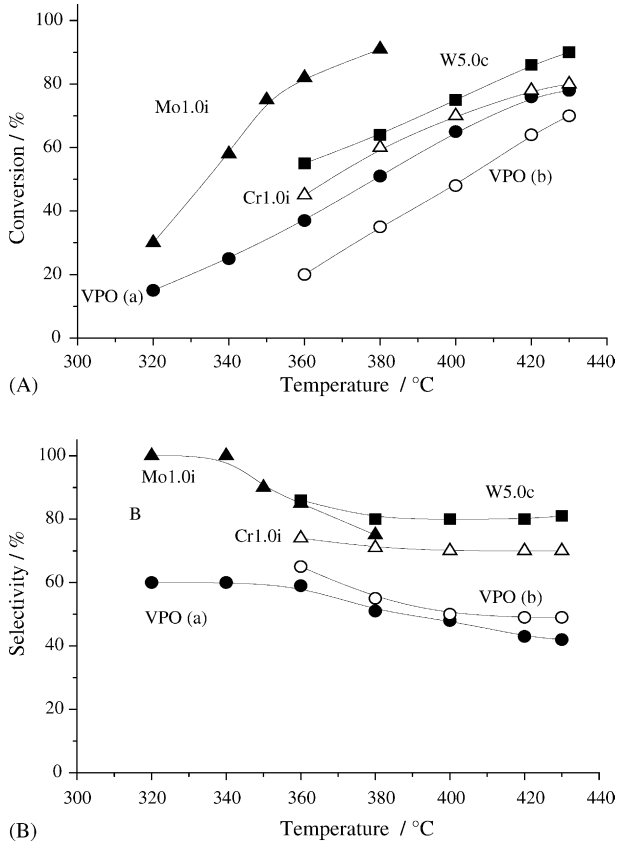

Fig. 2. Catalytic behavior of the best promoted catalysts and VPO bases used for impregnation: (A) catalytic activity and (B) selectivity to maleic anhydride. Feed stream 1.5% n-C_4H_{10} in air, GHSV = 900 h^{-1}.

a FWHM of 20 cm^{-1}. The measured FWHM of all the promoted catalysts varied between 24 and 35 cm^{-1}. The broadening of this signal is due to the presence of isolated V^{5+} centers located in the pyrophosphate lattice. This is in agreement with the results obtained in a joint work between our group and Volta's research team [25]. In that work it was determined by nuclear magnetic resonance that cobalt-promoted catalysts, after 500 h on stream, contained small amounts of dispersed V^{5+}.

3.4. Acetonitrile adsorption

The important role of the Lewis acidity has been acknowledged by various authors [4–7,12,26,27]. The Lewis sites would be useful to facilitate the paraffin activation and the subsequent hydrogen extraction to generate the olefin and the diolefin. Their role is also mentioned in the subsequent step of oxygen insertion [13,28]. Because of this, a direct relationship between acidity and activity could be expected as well as some additional incidence on selectivity, probably given by an optimal acidity value as reported by Carrara et al. [7].

Acetonitrile is a weak base, capable of discerning the presence of Lewis sites of different strength. When this base interacts with very strong Lewis sites such as $AlCl_3$, the CN stretching vibration shifts 74 cm^{-1} from its frequency in the

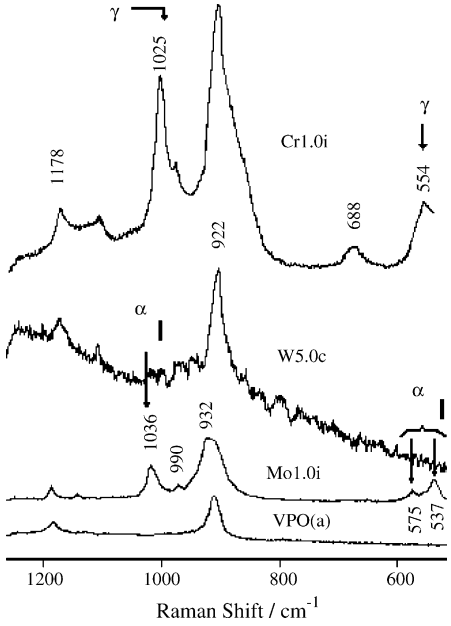

Fig. 3. Raman spectra of the best catalysts and the VPO(a) base γ-$VOPO_4$ bands: 1025, 990 and 554 cm^{-1} and α_I-$VOPO_4$ bands: 1036, 990, 575 and 537 cm^{-1} [19,20].

liquid phase (2252 cm^{-1}). A similar shift was observed in promoted catalysts, indicating the presence of very strong Lewis sites. The adsorption of acetonitrile on Mo1.0i at room temperature and after evacuation at higher temperatures is shown in Fig. 4. Note the development of an intense band at 2325 cm^{-1} indicative of acetonitrile adsorption on

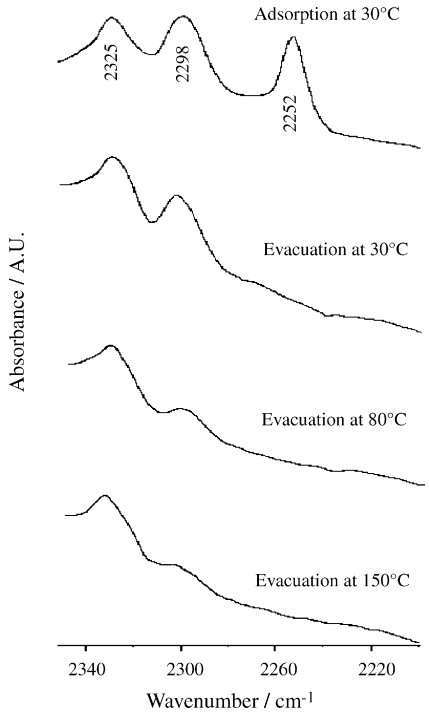

Fig. 4. FTIR spectra of ACN adsorbed on Mo1.0i. ν-CN = 2252 cm^{-1} (physisorbed); Fermi resonance = 2298 cm^{-1} and ν-CN_{ads} = 2325 cm^{-1} (very strong Lewis acid site).

Table 3
Redox properties, acidity and catalytic behavior of the best catalysts

Catalysts	M/V[a] × 10^2	T_{80}[b]	S_{80}[b]	S_{BET} ($m^2\ g^{-1}$)	$VOPO_4$[c]	V^{5+} (cm^{-1})[d]	ACN (μmol m^{-2})	$I(2325)/I(2298)$[e] evacuation 30 °C
VPO	–	445	50	28.2	NO	21	0.07	–
Mo1.0i	1.8	358	84	22.0	α_I	28	1.06	0.6
Cr1.0i	3.6	427	70	46.2	DH, γ	28	0.39	1.2
W5.0c	5.1	410	80	26.2	NO	35	0.72	0.2

[a] Promoter (M)/vanadium (V) atomic ratio.
[b] Temperature and selectivity at 80% conversion.
[c] DH:$VOPO_4{\cdot}2H_2O$, α_I:α_I-$VOPO_4$, γ:γ-$VOPO_4$ detected by XRD and/or LRS.
[d] FWHM of the Raman signal at 923 cm^{-1} (ν P–O–P), broadening due to isolated V^{5+} centers.
[e] Intensity ratio of the FTIR bands corresponding to very strong Lewis acid sites, 2325 cm^{-1} and to "Fermi resonance", 2298 cm^{-1}, after evacuation at 30 °C.

very strong Lewis acid sites. Its intensity is little affected by evacuation at 150 °C.

The amount of chemisorbed acetonitrile on all the catalysts varied between 0.01 and 1.42 μmol of ACN m^{-2}. The group of W- and Mo-promoted catalysts adsorbed the largest amounts, the values being between 0.51 and 1.42 μmol of ACN m^{-2}. In the Cr series, the Cr1.0i adsorbed 0.39 μmol of ACN m^{-2}. All the rest of the Cr-containing catalysts and the unpromoted VPOs only adsorbed between 0.01 and 0.10 μmol of ACN m^{-2}. The Mo1.0i catalyst presents the highest ACN chemisorption value which can be related to its high activity and selectivity. Likewise, the high activity of W-impregnated catalysts can also be explained by their high concentration of acid sites.

3.5. Redox properties, acidity and catalytic behavior

Table 3 shows the data pertaining to the best catalysts and the base VPO used for impregnation. This compilation was made trying to highlight the connection among the presence of dispersed V^{5+}, acidity and catalytic properties. The catalytic behavior is rapidly appreciated by looking at the third and fourth columns. They all contain V^{5+} sites dispersed in the pyrophosphate matrix while V^{5+} phases detected by XRD and/or Raman spectroscopy are only present in the Cr- and Mo-promoted solids (columns 6 and 7 of Table 3). The best catalysts contain very strong Lewis acid sites in varying proportions as indicated by the IR band appearing at 2325 cm^{-1} and indirectly by the total amount of chemisorbed acetonitrile (column 8 of Table 3). The $I(2325)/I(2298)$ ratio has been used to give an approximate estimate of the Lewis site concentration in a previous work [7,27].

Note that the less acidic VPO did not retain any acetonitrile adsorbed on very strong Lewis acid sites, while the promoted formulations retained the 2325 cm^{-1} band in varying proportions. This is symptomatic of the need to strike an adequate balance between the concentration of acid and redox sites.

4. Conclusions

- Starting from a single crystalline form of precursor ($VOHPO_4{\cdot}1/2H_2O$), the unpromoted catalyst is only made up of crystalline vanadyl pyrophosphate, while several promoted formulations contain V^{5+} phases detected through XRD and/or Raman spectroscopy.
- No memory effect between precursor and catalyst structures was observed in the 18 formulations. Neither was a correspondence found between stacking fold disorder and the addition of promoters.
- Molybdenum is the only promoter that increased the exposure of the [2 0 0] plane which contains the active sites for this reaction. This partially explains why Mo1.0i is the most active catalyst with high selectivity.
- The best catalysts contain dispersed V^{5+} centers and very strong Lewis acid sites and their concentrations seem to vary from one formulation to the other. Looking at the whole series of catalysts prepared, there seems to be an optimal balance between concentration of acid and redox centers to achieve the best possible yield for the oxidation of *n*-butane to maleic anhydride. In any case, a method is still needed to exactly quantify both the redox and acid sites concentrations in order to find clues allowing the optimization of the catalyst preparation.

In brief, the promoting effect of Cr, Mo and W seems to be connected with the generation of V^{5+} sites close to the abundant V^{4+} center of the pyrophosphate structure and to increase the concentration of very strong Lewis acid sites by creating surface defects. It cannot be discarded, however, that the presence of trace amounts of either element at the surface level may contribute to the C–H bond breaking of the starting paraffin. And, since this is the rate-determining step, increase the catalytic activity.

Acknowledgments

The authors wish to acknowledge the financial support received from UNL and CONICET. They are also grateful to the Japan International Cooperation Agency (JICA) for the donation of the major instruments used in this study. Thanks are finally given to Prof. Elsa Grimaldi for the English language editing.

References

[1] N. Harrouch Batis, H. Batis, A. Ghobel, Appl. Catal. A: Gen. 147 (1996) 347.
[2] G. Hutchings, Appl. Catal. 72 (1991) 1.
[3] Y. Takita, K. Tanaka, Sh. Ichimaru, Y. Mizihara, Appl. Catal. A 103 (1993) 281.
[4] D. Ye, A. Satsuma, A. Hattori, T. Hattori, Y. Murakamii, Catal. Today 16 (1993) 113.
[5] M. Abon, J.M. Herrmann, J.C. Volta, Catal. Today 71 (2001) 121.
[6] V. Zazhigalov, J. Haber, J. Stoch, I. Bacherkova, G. Komashko, A. Pyatniskaya, Appl. Catal. A: Gen. 134 (1996) 225.
[7] C. Carrara, S. Irusta, E. Lombardo, L. Cornaglia, Appl. Catal. A 217 (2001) 275.
[8] G. Hutchings, R. Higgins, J. Catal. 162 (1996) 153.
[9] W. Ji, L. Xu, X. Wang, Z. Hu, Q. Yan, Y. Chen, Catal. Today 74 (2002) 101.
[10] R. Mc Cormick, G. Alptekin, A. Herring, T. Ohno, S. Dec, J. Catal. 172 (1997) 160.
[11] P. Mars, D.W. van Krevelen, Chem. Eng. Sci. 3 (1954) 160.
[12] G. Centi, F. Trifirò, J. Ebner, V. Franchetti, Chem. Rev. 88 (1988) 55.
[13] Y. Zhang-Lin, M. Forissier, R.P. Sneeden, J.C. Védrine, J.C. Volta, J. Catal. 145 (1994) 267.
[14] J.C. Volta, Top. Catal. 15 (2001) 121.
[15] B. Weckhuysen, R. Schoonheydt, Catal. Today 51 (1999) 223.
[16] B. Grzybowska, Pol. J. Chem. 77 (2003) 627.
[17] K. Kourtakis, P. Gai, J. Mol. Catal. A: Gen. 220 (2004) 93.
[18] J. Bartley, I. Ellison, A. Delimitis, C. Kiely, A. Isfahani, C. Rhodes, G. Hutchings, Phys. Chem. Chem. Phys. 3 (2001) 4600.
[19] E. Kesteman, M. Merzouki, B. Taouk, E. Bordes, R. Contractor, in: G. Poncelet et al. (Eds.), Preparation of Catalysis VI, Stud. Surf. Sci. Catal. 91 (1995) 707.
[20] G. Centi, Catal. Today 16 (1993) 5.
[21] G. Sola, B. Pierini, J. Petunchi, Catal. Today 15 (1992) 537.
[22] E. Bordes, Catal. Today 1 (1987) 499.
[23] V. Guliant, J. Benziger, S. Sunderesan, I. Wachs, J. Jehng, J. Roberts, Catal. Today 28 (1996) 275.
[24] F. Ben Abdelouhab, R. Olier, N. Guilhaume, F. Lefevre, J.C. Volta, J. Catal. 134 (1992) 151.
[25] L. Cornaglia, S. Irusta, E.A. Lombardo, M.C. Durupty, J.C. Volta, Catal. Today 78 (2003) 291.
[26] G. Busca, G. Centi, F. Trifiro, V. Lorenzelli, J. Phys. Chem. 90 (1986) 1337.
[27] L.M. Cornaglia, E.A. Lombardo, J.A. Anderson, J.L. García Fierro, Appl. Catal. A 100 (1993) 37.
[28] B. Schiøtt, K.A. Jørgensen, R. Hoffman, J. Phys. Chem. 95 (1991) 2297.